Environmental Earth Sciences (2022) 81:107
https://doi.org/10.1007/s12665-022-10229-8

ORIGINAL ARTICLE

Stress–strain behavior of modified expansive clay soil: experimental measurements and prediction models

Anoosheh Iravanian[1] · **Youssef Kassem**[1,2] · **Hüseyin Gökçekuş**[1]

Received: 23 March 2021 / Accepted: 22 January 2022 / Published online: 7 February 2022

Abstract

Building on expansive soil is risky due to its high compressibility, low shear strength, and differential settlement. This study evaluates the potential of the use of sodium hydroxide (NaOH) as an additive to improve the stability of clay. For this research, the compaction properties namely Dry Density, Optimum Moisture Content, Atterberg Limits, and Unconfined Compressive Strength were performed on soil samples prepared with different percentages of NaOH (0%, 5%, 10%, 15%, and 20%). In this work, the clay sample was obtained from a highway project site near the Haspolat village in the eastern suburb of North Nicosia, Cyprus. No works of such have been done in the area. The results indicated that NaOH can be added to improve the engineering properties of the soil. Moreover, this paper presents a comparative study between an empirical equation (Quadratic model (QM)), Multilayer Feed-Forward Neural Network (MFFNN), Cascade Feed-forward Neural Network (CFNN), Radial Basis Neural Network (RBNN), and Elman neural network (ENN)) and multiple linear regression (MLR) for modeling the stress–strain behavior of CS15 (contains 85% of soil and 15% of NaOH). The coefficient of determination, root mean squared error, mean absolute error, Nash–Sutcliffe efficiency, and Willmott's index of the agreement were used to select the best predictive model. The results indicate that all the developed models are expedient in predicting the stress–strain behavior of treated soil. Furthermore, the findings demonstrated that the QM model performed well and presented high accuracy in modeling the stress–strain behavior.

Keywords Quadratic model · Artificial intelligence models · Multiple linear regressions · Soil stabilization · Stress–strain behavior · Sodium hydroxide

Introduction

Soil with high contents of clay minerals like Montmorillonite and Verimculite is usually difficult to deal with, due to undesirable properties like absorbing high amounts of water, having low shear strength, and performing high compressibility. These types of clay are called expansive soils due to the swelling and shrinkage properties they display when water is present or absent, respectively (Gokul et al. 2020; Mohanty 2018). Thus, it is necessary to stabilize these soils to enhance the engineering properties of the soil such as mechanical strength, permeability, compressibility, durability, and plasticity. In the literature, chemical stabilization of soil has been practiced to improve the engineering characteristics and enhance the load-bearing capacity of weak soil (Coudert et al. 2019; Jayawardane et al. 2020).

In general, stabilization is referred to chemical improvements in the properties of the soil by adding soil additives. Several geotechnical research has been carried out on the effect of adding soil additives on the engineering properties of the soil. For example, Rai et al. (2020) investigated the effect of waste marble powder and magnesium phosphate cement on the properties of the soil. They found that marble powder and magnesium phosphate cement improved the

✉ Youssef Kassem
youssef.kassem1986@hotmail.com;
yousseuf.kassem@neu.edu.tr

Anoosheh Iravanian
anoosheh.iravanian@neu.edu.tr

Hüseyin Gökçekuş
huseyin.gokcekus@neu.edu.tr

[1] Department of Civil Engineering, Civil and Environmental Engineering Faculty, Near East University, 99138 Nicosia (via Mersin 10, Turkey), Cyprus

[2] Department of Mechanical Engineering, Faculty of Engineering, Near East University, 99138 Nicosia (via Mersin 10, Turkey), Cyprus

stability of the soil. Gokul et al. (2020) experimentally examined the effect of Ground Granulated Blast Furnace Slag (GGBFS) on the stability of the clayey soil. Their results showed that the UCS of the stabilized soil was increased by increasing the percentage of GGBFS. Tanegonbadi and Noorzad (2017) improved the stability of the clay soil using Lignosulfonate. They found that the Lignosulfonate-treated soil increased the Unconfined Compressive Strength (UCS) and stiffness of the soil without leading to a considerable brittle behavior based on the stress–strain curves of UCS tests. Ghadir and Ranjbar (2018) determined the compressive strength and compared the mechanical performance of clay soil-geopolymer and clay soil-ordinary Portland cement. They found that geopolymer treatment and Portland cement were more efficient in dry conditions and wet environments, respectively. Furthermore, adding a chemical additive such as sodium hydroxide (NaOH) into clay soil will improve clayey soil characteristics such as undrained shear strength, Unconfined Compressive Strength, USC, and liquid limit (Neeladharan et al. 2007; Hu et al. 2009; Modmoltin and Voottipruex 2009; Rashad and Zeedan 2011; Davoudi and Kabir 2011; Cristelo et al. 2012; Phummiphan et al. 2016; Parhi et al. 2017; Miao et al. 2017; Fasihnikoutalab et al. 2019; Ghavami et al. 2020; Murmu et al. 2020). Generally, NaOH is one of the important inorganic chemical raw materials that are commonly utilized in industrial manufacturing, wood and paper products, the food industry, and many other fields (Hassan et al. 2019; Madhav et al. 2018). Recently, NaOH is applied to reduce the stabilization cost of the material used for road and building construction by mixing the soil with the required amount of NaOH (Phummiphan et al. 2017). The reviewed studies have shown that the UCS value was significantly influenced by sodium hydroxide concentration in the mixture.

Given the fact that stabilized soil behavior can be a challenge in a geotechnical context, the investigation of the stress–strain behavior of soils is important for evaluating safety in geotechnical engineering such as hazard prevention during tunneling and groundwater-soil interaction in excavations (Zhang et al. 2017; Lyu et al. 2019, 2020). The behavior of stress–strain graphs of these samples show high nonlinearity (Zheng et al. 2020). Several empirical models including artificial neural networks, supervised Learning Methods and mathematical have been used to predict engineering properties of soil, concrete, and so on (Nassr et al. 2018; Zheng et al. 2020; Molaabasi et al. 2019; Debnath and Dey 2016; Yao et al. 2018; Ahmad et al. 2020; Dutta et al. 2020, Ahmad et al. 2021). For example, Zheng et al. (2020) predicted the stress–strain behavior using the Long Short-Term Memory deep learning method, feed-forward neural network, and feedback neural network. The results indicated that the LSTM deep learning method was superior in predicting the stress–strain behavior with reported values of 8.25, 6.1, and 0.955 for the parameters of the mean absolute error (MAE), the mean absolute percentage error (MAPE), and R-squared. Debnath and Dey (2016) utilized a feed-forward back-propagation neural network with various learning algorithms to estimate the peak shear stress along with the cohesive soil–geosynthetic interface. It was observed that the Bayesian regularization back-propagation learning algorithm has the lowest statistical error compared to other learning algorithms. Dutta et al. (2020) evaluated the performance of three techniques including techniques ANN, Multiple regression analysis, and M5P model tree for the prediction of clay friction angle. The results indicated that the developed ANN model was superior to the one obtained using MRA and to M5P model tree technique, which is based on statistical parameters. Moreover, Table S1 as supplementary material captures some of the notable work that has been conducted in this field (Johari et al. 2011; Javadi et al. 2012; Kohestani and Hassanlourad 2016; Asr et al. 2018; MolaAbasi et al. 2019; Pham et al. 2022; Zhang et al. 2021; Kim et al. 2022). As the parameters of the current research show, some have had a broad scope, modeling the stress behavior of a general group of soils, and some focused on less widely used soil treatment methods aiming to understand the effect of specific stabilizers on soil behavior.

To the best of our knowledge, there are no studies in the literature about the effect of NaOH on the engineering properties of clay soil in the Northern part of Cyprus. In general, due to swelling minerals such as smectite or illite, clay soils may cause severe damage to the foundations and cracks on the surface of a structure, particularly when the soil is exposed to wetting and drying conditions (Shalabi et al. 2017). According to Abdeh (2018), swelling clay formations are mostly found in the western and northern parts of Nicosia, Cyprus. The reduction in strength and high expansion takes place in these areas due to the increase in water content in clay soil after wet winters. Thus, utilizing additives and chemical stabilizers can improve the engineering properties of the soil.

The purpose of this paper is to investigate the effect of NaOH on the engineering properties of clay soil. Clay soil-NaOH blends were mixed in various percentages (0.5, 10, 15, and 20%). The compaction properties (Atterberg's limits, Maximum Dry Density, Optimum Moisture Content, and Unconfined Compressive Strength) of untreated and treated soil were measured. In this study, each test was repeated three times and then the average was determined to reduce the experimental error. Moreover, according to the authors' review, no studies had evaluated the accuracy of the Quadratic model (QM) to predict the stress–strain behavior of the NaOH-soil mixture. The present work, therefore, consists of

establishing a stress–strain behavior estimation model that aims to estimate stress–strain behavior of treated soil from more easily measured variables obtained at the same instant as the desired forecast. Based on the analysis of the experimental results, the accuracy of the Quadratic model (QM) for modeling the stress–strain behavior of NaOH treated clay soil. Moreover, the proposed model (QM) was compared with the most common machine learning models such as MFFNN, CFNN, RBFNN, and ENN, and MLR to show the predictive accuracy of the proposed model.

Materials and methods

In this section, the preparation of the clay soil-NaOH mixtures and measurement of their properties according to standards are discussed. Figure 1 illustrates the analysis procedure of the present study.

Soil characterization

The soil used in the present study was collected from Haspolat village in the eastern suburb of North Nicosia, Cyprus. The color is gray and it is originated from mudstone. The soil samples were first dried at 50 °C in an oven, and then manually crushed and sieved through a sieve with openings of 2.35 mm to remove the unwanted organic particles and gravel fraction. The particle size distribution of soil was then investigated using the Hydrometer test following the ASTM D422 standard.The tests for determining the physical properties of the selected soil in terms of Atterberg limits (liquid limit, LL, plastic limit, PL), specific gravity, grain size distribution, and soil classification were done according to the ASTM D 4318, the ASTM D 422 and the Unified Soil Classification System, respectively, as shown in Table 1. Moreover, the standard Proctor compaction test following ASTM D 698 was conducted to estimate the maximum dry density (ρ_{max}) and the optimum moisture content (OMC) of the soil. In this work, each test was repeated three times and the average was determined to reduce the experimental error. It was found that the values of ρ_{max} and OMC are 1.72 g/cm^3 and 20%, respectively.

Sodium hydroxide (NaOH) pellets

Sodium hydroxide pellets are inorganic compounds. This material is also known as caustic soda with a chemical formula of NaOH. This inorganic compound consists of sodium cations Na^+ and hydroxide anions OH^-. Sodium hydroxide is a highly caustic base and is used in industries such as the manufacture of pulp and paper, textiles, drinking water, soaps and detergents, and as a drain cleaner.

Preparation of mixtures

In this study, a series of mixtures were prepared by mixing the clay soil with various percentages of NaOH. The percentage of NaOH added to the soil were varying from 0 to 20% by weight.

In the present study, five different mixtures of clayey soil (CS) with a different percentage of NaOH (CS0, CS5, CS10, CS15, and CS20) were prepared. These mixtures were prepared as follows:

- CS0 contains 100% of soil and 0% of NaOH
- CS5 contains 95% of soil and 5% of NaOH
- CS10 contains 90% of soil and 10% of NaOH
- CS15 contains 85% of soil and 15% of NaOH
- CS20 contains 50% of soil and 50% of NaOH

In this experimental work, the maximum dry density, and the optimum moisture content were measured for all samples. Then, the samples were compacted at their maximum dry density and optimum moisture content to be tested for their unconfined compressive strength. The unconfined compression test apparatus was used with a load ring capacity of 6.6 kN to analyze the stress–strain behavior of the samples. The monitoring of percentage strain during the test was done using a digital transducer connected to a computer for measuring the deformation of the sample by the accuracy of 0.01 mm. The heights of samples were measured before each test using a digital caliper. The load was transferred to the sample with a ratio of 1 mm/min.

Empirical models

Artificial neural networks (ANN)

Machine learning models are used as alternative tools to describe a complex system (Livingstone 2009; Keat et al. 2015; Kassem et al. 2019, 2018; Gökçekuş et al. 2020). They are utilized in a wide variety of applications in engineering and science. In this study, four empirical models [Multilayer feed-Forward Neural Network (FFNN), Cascade Forward Neural Network (CFNN), Radial Basis Function Neural Network (RBFNN), and Elman neural network (ENN)] are developed to predict the stress–strain behavior of the soil. In this work, the value of clay soil content, NaOH content, axial strain, area, and force are used as explanatory input variables. The data are divided into training and testing groups and the results by the models are compared with each. In this study, the training was done using data for 0, 5, 10, and 20% NaOH treated soil, and the developed model was used to predict the stress–strain plot for 15% NaOH treated soil, and then compared with the stress–strain plot obtained by

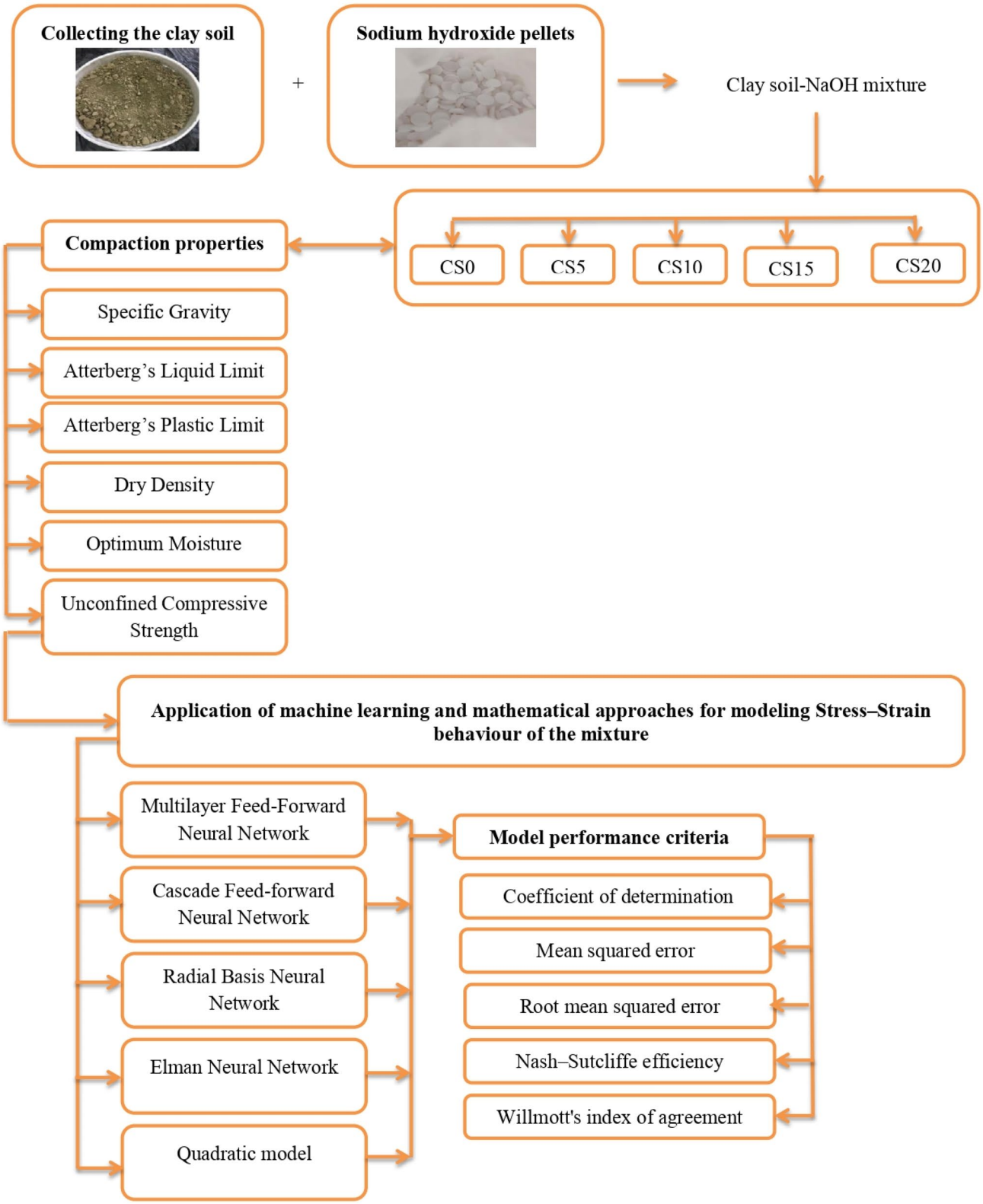

Fig. 1 Flowchart of analysis procedure in the present study

Table 1 Engineering properties of clay soil

Property	Unit	Value
Specific gravity	–	2.55
Atterberg limits		
LL	%	68
PL	%	32
PI	%	36
Grain fractions		
Clay	%	64
Silt	%	33
Sand	%	3
Soil classification	–	CH

performing laboratory test on actually prepared 15% NaOH treated soil.

Multilayer feed-forward neural network (MFFNN) The MFFNN consists of three layers (input layer, hidden layer, and output layer). The number of neurons and the number of hidden layers should be carefully selected because they affect the accuracy of training. TRAINLM is utilized as a training function. Also, Mean squared error (MSE) is estimated to find the best performance of the training algorithm. The declining gradient of the back-propagation algorithm is utilized to reduce the value of MSE between the actual and estimated output. The description of the developed model was given in Kassem and Gokcekus (2021). Figure 2 illustrates the explanation process of the proposed MFFNN method.

Cascade feed-forward neural network (CFNN) CFNN represents a static neural network where the signals move in the forward direction only (Alkhasawneh and Tay 2018). It is similar to a feed-forward neural network but it contains a connection from the input and every previous layer to the layers of the following layer (Hedayat et al. 2009; Zheng et al. 2020). The advantage of this model is that it can show the nonlinear relationship without eliminating the linear relationship between input and output. The optimum number of neurons is based on the minimum value of RMSE. The description of the developed model was given in Kassem and Gokcekus (2021). Figure 3 describes the steps of the proposed model (CFNN).

Radial basis neural networks (RBFNN) RBFNN is a feed-forward network, which consists of one input layer, one hidden layer, and one output layer. It is used radial basis functions as activation functions (Barati-Harooni and Najafi-Marghmaleki 2016). Speed and efficiency are the most important advantages of RBFNN models compared to other multi-layer perceptron models due to their simple structure. The description of the developed model was given in Kassem and Gokcekus (2021). Figure 4 illustrates the steps of the proposed model (RBFNN).

Elman neural network (ENN) The ENN is a simple type of recurrent neural network. It includes four main layers namely, the input layer, context layer, hidden layer, and the output layer (Yu et al. 2019). The main ENN structure is similar to the multi-layer neural network. As mentioned previously, there is a context layer in ENN; the inputs of this layer come from outputs of the hidden layer, which were utilized to store the hidden layer's output values of the previous time (Yu et al. 2017; Ren et al. 2018).

Quadratic model (QM)

The QM is a mathematical model that can be simultaneously model the input variables and output variables affected by input variables. The aim of using this model is to estimate the degree of effect of the input variables (percentage of clay soil (*CSc*), percentage of NaOH (*NaOHc*), axial strain (*AS*), area (A), and force (F)) on the output parameter (deviator stress (*q*)) of the treated soil. Equation (1) presents the relationship form between the input parameters and output parameters.

$$q = f(PCS, PNaOH, LS, \mathrm{A}, \mathrm{F}). \tag{1}$$

Based on the actual data, regression analysis was carried out by the following quadratic polynomial model:

$$Y = \beta_0 + \sum_{i=1}^{n} \beta_i x_i + \sum_{i=1}^{n} \beta_{ii} x_i^2 + \sum_{i}^{n-1} \sum_{i=i+1}^{n} \beta_{ij} x_i x_j, \tag{2}$$

where Y is the predicted response, β_0 a constant, β_i the linear coefficient, β_{ii} the squared coefficient, and β_{ij} the cross-product coefficient, n is the number of factors, x_i and x_j are the independent variables.

Multiple linear regressions (MLR)

MLR is a classical method, which attempts to model the correlation between independent variables (x) and dependent (y). It explores how the dependent and independent variables are correlated. The MLR model is

$$Y = \beta_0 + \beta_1 x_1 + \cdots + \beta_i x_i i = 1, 2 \ldots n, \tag{3}$$

where Y is the predicted response, β_0 a constant, β_i the intercept and x_i where $i = 1,2,..,n$, denotes the explanatory or independent variables.

Model performance criteria

Coefficient of determination, root mean squared error and mean absolute error were used to measure the estimation success of the models. The following equations were used for evaluation.

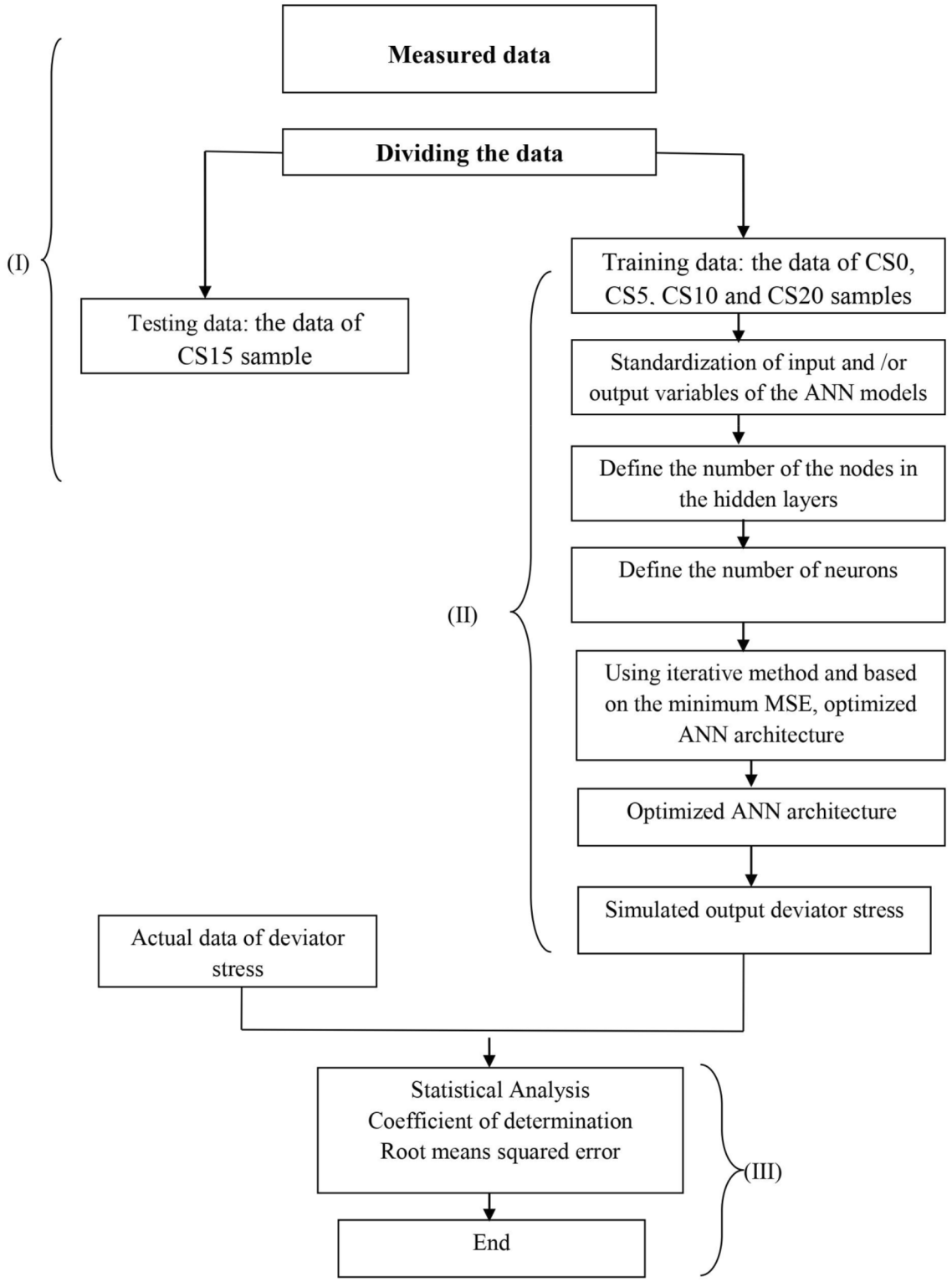

Fig. 2 The proposed algorithm of predicting stress–strain behavior of the soil using MFFNN

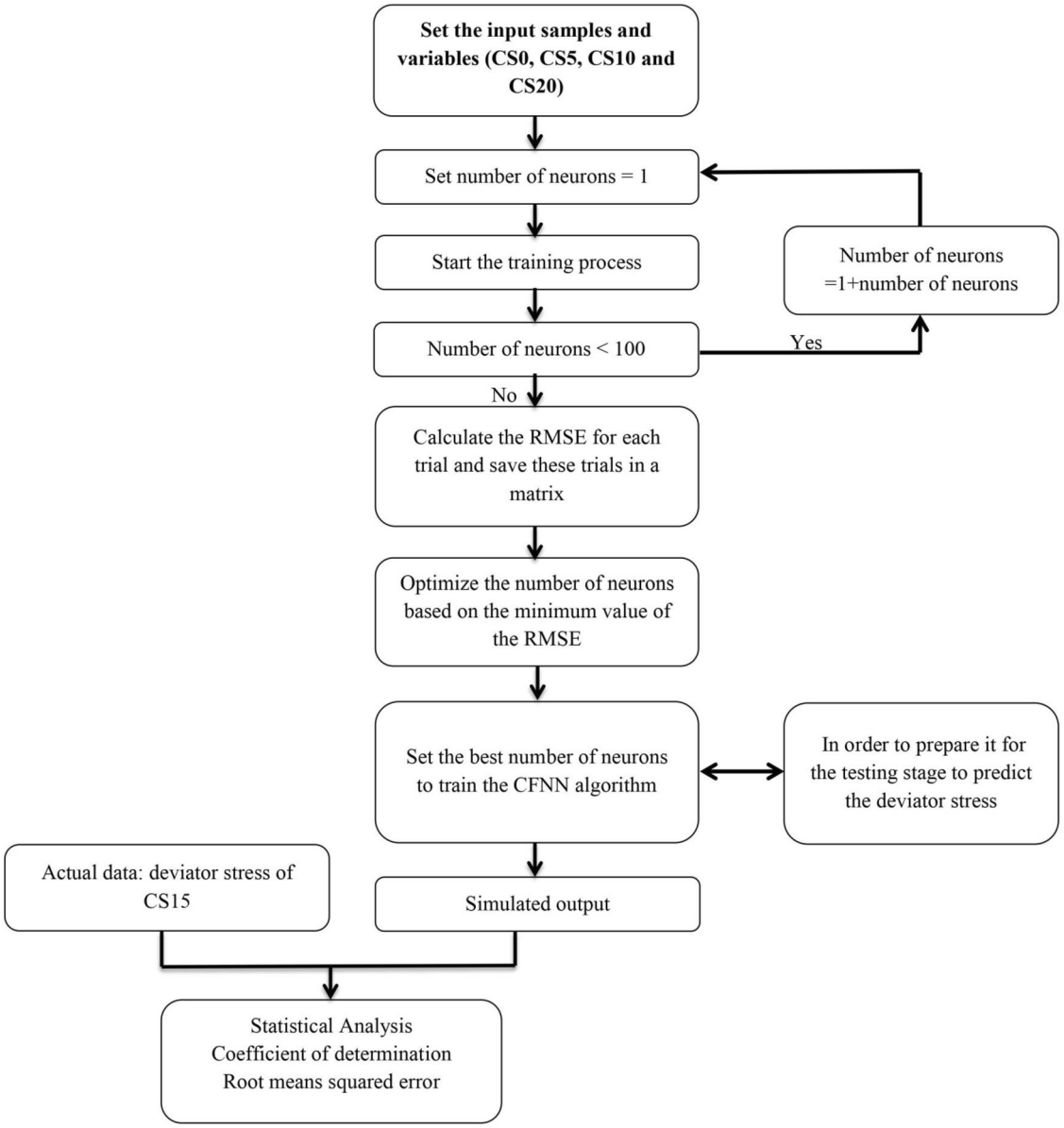

Fig. 3 The proposed algorithm of predicting stress–strain behavior of the soil using CFNN

Coefficient of determination (R^2)

$$R^2 = 1 - \frac{\sum_{i=1}^{n} \left(a_{a,i} - a_{p,i}\right)^2}{\sum_{i=1}^{n} \left(a_{p,i} - a_{a,\text{ave}}\right)^2}. \quad (4)$$

Mean squared error (MSE)

$$\text{MSE} = \frac{1}{n} \sum_{i=1}^{n} \left(a_{a,i} - a_{p,i}\right)^2. \quad (5)$$

Root mean squared error (RMSE)

$$\text{RMSE} = \sqrt{\frac{1}{n} \sum_{i=1}^{n} \left(a_{a,i} - a_{p,i}\right)^2}. \quad (6)$$

Mean absolute error (MAE)

$$\text{MAE} = \frac{1}{n} \sum_{i=1}^{n} \left|a_{a,i} - a_{p,i}\right|. \quad (7)$$

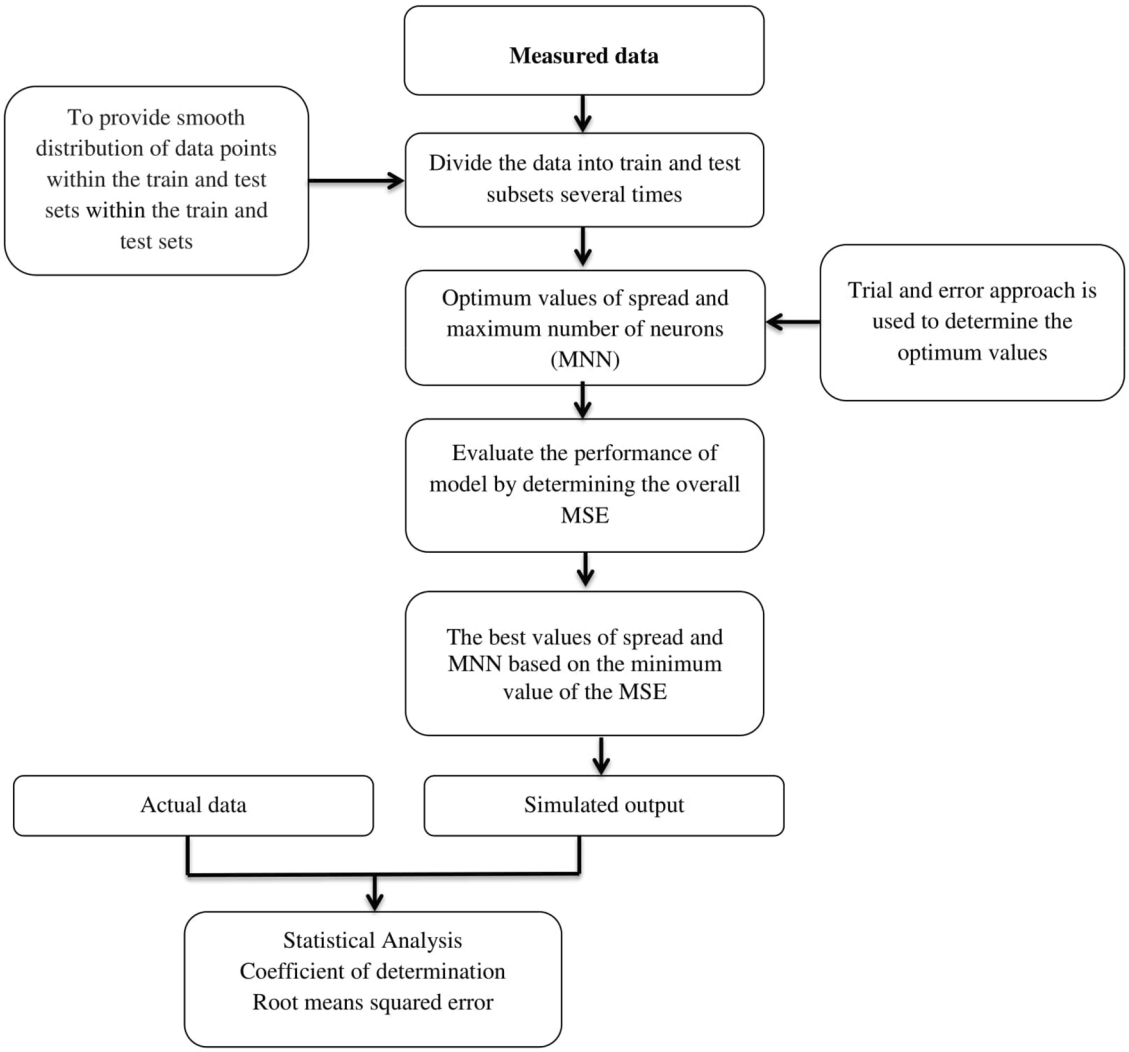

Fig. 4 The proposed algorithm of predicting stress–strain behavior of the soil using RBFNN

Nash–Sutcliffe efficiency (NSE)

$$\mathrm{NSE} = 1 - \frac{\sum_{i-1}^{n} \left(a_{a,i} - a_{p,i}\right)^2}{\sum_{i-1}^{n} \left(a_{a,i} - a_{a,\mathrm{ave}}\right)^2}. \tag{8}$$

Willmott's index of agreement (*d*)

$$d = 1 - \frac{\sum_{i-1}^{n} \left(a_{a,i} - a_{p,i}\right)^2}{\sum_{i-1}^{n} \left(\left|a_{p,i} - a_{a,\mathrm{ave}}\right| + \left|a_{a,i} - a_{a,\mathrm{ave}}\right|\right)^2}, \tag{9}$$

where n is the number of data, $a_{p,i}$ is the predicted values, $a_{a,i}$ is the actual values, $a_{a,\mathrm{ave}}$ is the average actual values and i is the number of input variables.

Results and discussion

Soil stabilization and characterization tests

Atterberg limits

Figure 5 shows the results of Atterberg Limits in terms of liquid limit (LL), plastic limit (PL), and plasticity index

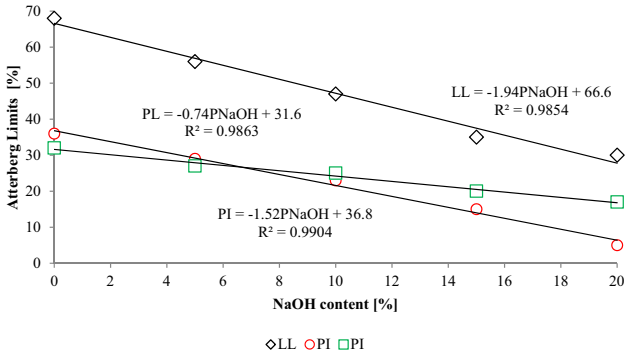

Fig. 5 Atterberg limits of Clay soil-NaOH mixture

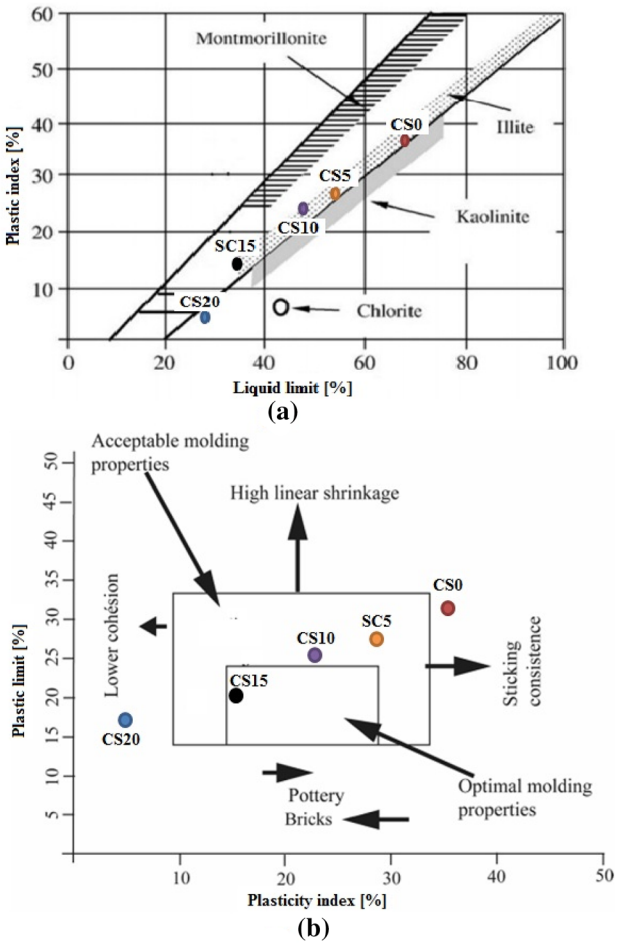

Fig. 6 Position of soil-NaOH samples; **a** on the Holtz and Kovacs diagram (Holtz and Kovacs 1981) and **b** Casagrande diagram

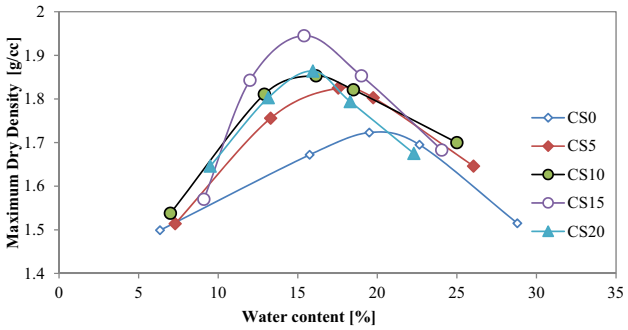

Fig. 7 Compaction curves of the clay soil at different NaOH content

Table 2 Results of ρ_{max} and OMC for clay soil-NaOH samples

Sample	OMC [%]	ρ_{max}[g/cc]
CS0	20	1.72
CS5	18	1.82
CS10	16	1.85
CS15	15	1.94
CS20	16	1.80

(PI) tests of the five samples. Additionally, the results of the Atterberg limits are plotted on the Holtz and Kovacs diagram and workability chart as shown in Fig. 6. The Liquid Limit (LL), Plastic Limit (PL), and Plasticity Index (PI) following ASTM D4318 are within the range of 68–30%, 32–17% and 36–5%, respectively. It was found that all Atterberg parameters, LL, PL, and PI, decreased almost linearly with the increase in NaOH content.

Except for the CS20, which was in the moderate plastic region, all clay soil-NaOH samples were found in the highly plastic region, as the reference clay sample as shown in Fig. 3a. CS0, CS5, CS10, and CS15 samples were found in the Illite clay region. It shows that these samples have higher LL and PI values than CS20. CS10 has acceptable extrusion properties similar to the CS5 sample, whereas the CS15 sample has optimal properties. CS20 demonstrates lower cohesion and is an outlier as shown in Fig. 3b. In general, according to Murray (2007), the plasticity value of the soil is an essential parameter utilized in estimating the application of the clay body. In clay soil-NaOH, PL value is within the range of 32–17%. According to Monterio and Vieira (2004), the high value of PL is associated with greater mechanical strength. Furthermore, Siddiqui and Osman (2012) concluded that the differences in PL of the soil samples are usually understandable from the particle size distribution data.

Unconfined compressive strength and optimum compaction

It is well known that the estimation of shear strength of the soil is essential in civil engineering for various applications like highway and airfield design, the stability of slopes and cuts, and the design of coastal structures. In this study, Unconfined Compressive strength (UCS) tests were carried out on samples with 0%, 5%, 10%, 15%, and 20% NaOH contents, compacted at their at ρ_{max} and OMC, which were obtained from the standard Proctor compaction curves. Figure 7 shows the compaction curves of the clay soil-NaOH at different NaOH contents. It was observed that the sample with 15% NaOH has the maximum value of ρ_{max} and minimum value of OMC comparing to other samples (see Table 2).

The unconfined compression test apparatus was used with a load ring capacity of 6.6 kN. The monitoring of percentage strain during the test was done using a digital transducer connected to a computer for measuring the deformation of the sample by the accuracy of 0.01 mm. The height of samples was measured before each test using a digital caliper. The load was transferred to the sample with a ratio of 1 mm/min.

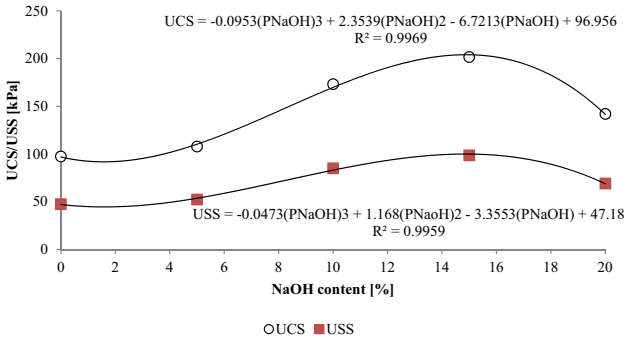

Fig. 8 Unconfined compressive strength (UCS) and undrained shear strength (USS) of the clay soil with NaOH content

Figure 8 illustrates the effect of various percentages of NaOH on the results of the UCS of the samples. Comparing with the sample without NaOH, the UCS of the sample with 15% NaOH increased from 97.5 to 201.7 kPa, i.e. 15% NaOH increased the UCS to peak value as shown in Fig. 8. Additionally, it was found that by increasing the NaOH content to 20% the value of UCS was reduced from 201.7 to 142.0 kPa. It was observed that the unconfined strength value increases 107% with the addition of 15% stabilizer, and the further addition of NaOH has an adverse effect on UCS and hence the shear strength of the soil. The witnessed strength gain can be described by the reaction of sodium hydroxide with the clay mineral. The alkaline attack changes the clay mineral lattice and results in producing sodium silicate and sodium aluminates. Further addition of NaOH is thought to disturb the clay mineral structure and therefore decrease the UCS. According to Das and Sobhan (2014) consistency/UCS correlation chart, the compacted untreated clay samples consistency can be classified as "firm" based on the obtained value of UCS, while the UCS of samples treated with 5%, 10%, and 20% NaOH classify them as "stiff" and with 15% NaOH as "very stiff".

Given that the undrained shear strength is independent of the confining pressure in saturated undrained clays, the shear strength at failure, τ_f, of the samples would be equal to the cohesion of them and could be calculated by dividing the failure stress by two (Das and Sobhan 2014).

Table 3 Statistical parameters of used variables

Data set	Variable	Explanation	SD	CV	Min	Max	Range	Unit
Training	CSc	Clay soil content	7.2	7.9	80.0	100.0	20.0	%
	NaOHc	NaOH content	7.2	86.5	0.0	20.0	20.0	%
	AS	Axial strain	3.3	74.8	0.0	13.3	13.3	%
	A	Area	33.4	2.5	1250.3	1405.8	155.5	mm^2
	F	Force	83.8	58.7	0.0	279.0	279.0	N
	q	Deviator stress	61.9	58.0	0.0	207.5	207.5	kPa
Testing	CSc	Clay soil content	0.0	0.0	85.0	85.0	0.0	%
	NaOHc	NaOH content	0.0	0.0	15.0	15.0	0.0	%
	AS	Axial strain	1.0	58.0	0.0	3.6	3.6	%
	A	Area	8.9	0.7	1332.6	1368.3	35.7	mm^2
	F	Force	57.7	29.5	− 19.0	240.0	259.0	N
	q	Deviator stress	42.8	29.5	− 14.1	178.9	193.0	kPa

It was found that the sample with 15% NaOH has the maximum average τ_f with a value of 99 kPa as shown in Fig. 8.

Artificial models

As mentioned previously, four neural network models were employed to predict the deviator stress (q) for clay soil-NaOH samples. Thus, the value of clay soil content, NaoH content, axial strain, area, and force are used as explanatory input variables. The data were divided into training and testing groups and the results by the models were compared with each. In this study, the training was done using data for 0, 5, 10, and 20% NaOH-treated soil, and the developed model was used to predict the stress–strain plot for 15% NaOH-treated soil, and then compared with the stress–strain plot obtained by performing laboratory test on actually prepared 15% NaOH treated soil. The summary statistics of the independent variables, which are considered as input and dependent variables (output), are given in Table 3.

A series of models were examined to estimate the optimum number of hidden layers (HL), the number of neurons (NN), and transfer function (TF) for the MFFNN, CFNN, and ENN models. It should be noted that the number of HLs and NNs in the MFFNN, CFNN and ENN models was determined by utilizing trial and error approaches. Based on the value of MSE, it was found that two hidden layers and ten neurons are selected as the best for the MFFNN model (5:1:1) with an MSE value of 6.20×10^{-6}. While it found that two hidden layers and five neurons were chosen as an optimum number for the CFNN model (5:2:1) with an MSE value of 274×10^{-6}. Also, it was observed that the ENN model (5:3:1) with ten neurons has the minimum MSE with a value of 2.26×10^{-6}.

Moreover, the 10-th order root of the input data was used instead of actual input data to provide better performance for the RBFNN model. This helps to smooth the variation of the input data points within a narrower range and this leads to better accuracy of the implemented model. Then, the data points were randomly divided into training and testing subsets. The random division was carried out several times to prevent the aggregation of data points in the desired domain of the problem and to provide a smooth distribution of data points within the training and testing sets. In general, the spread and the maximum number of neurons (MNN) are important parameters in the structure of RBFNN as the performance and accuracy of the implemented model are significantly affected by the values of these parameters. Similarly, the optimum values of these parameters were estimated by a trial and error approach. It was observed that the optimum values that provide the most accurate performance for the RBFNN model are 0.001 and 200 for the spread and MNN, respectively.

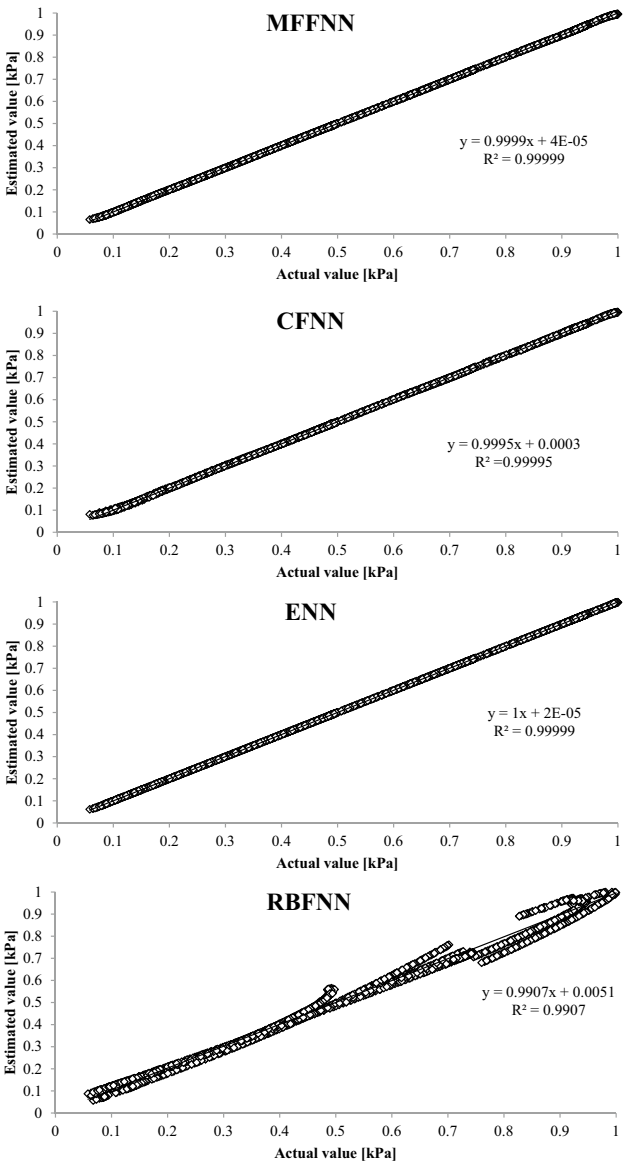

Fig. 9 Comparison between predicted data with actual data of deviator stress using various ANN models

Figure 9 illustrates the *R*-squared for training data of deviator stress for clay soil-NaOH mixtures. *R*-squared was used to evaluate the performance of artificial models. *R*-squared means the degree of the linear relationship between the observed and modeled values. The line is almost straight with a 45° angle and this proves the accuracy of the provided model. For the training phase, the R^2 value was found to be approximately 1 as shown in Fig. 6. The results obtained from the ANN models show that the use of ANN is enough to predict deviator stress for clay soil-NaOH mixtures.

Table 4 Analysis of variance of QM for deviator stress responses

Sources of variations	Degree of freedom	Sum of squares	Mean square	*F* value	*P* value
Model	14	150.104	10.7217	9.31*E*+08	0.00**
Linear	4	42.101	10.5253	9.14*E*+08	0.00**
CSc	1	0	0	0.2	0.658
AS	1	0	0	120.59	0.00**
A	1	0.012	0.0119	1,030,096	0.00**
F	1	0.913	0.9134	79,324,888	0.00**
Square	4	0	0	628.71	0.00**
CSc^2	1	0	0	43.26	0.00**
AS^2	1	0	0	267.68	0.00**
A^2	1	0	0	151.92	0.00**
F^2	1	0	0	515.35	0.00**
2-Way interaction	6	0.008	0.0013	114,305.7	0.00**
CSc × AS	1	0	0	0.86	0.353
CSc × A	1	0	0	37.21	0.00**
CSc × F	1	0	0	639.56	0.00**
AS × A	1	0	0	10.5	0.001**
AS × F	1	0	0	345.67	0.00**
A × F	1	0.002	0.0022	193,994.3	0.00**

*Significant at 5% level

**Significant at 1% level

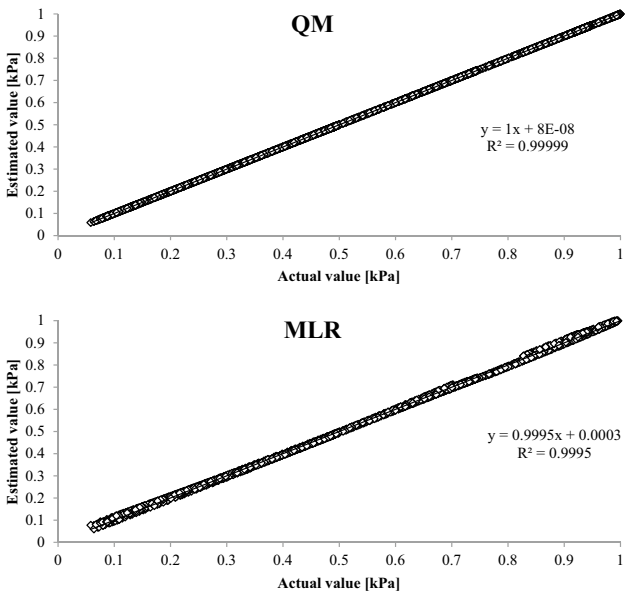

Fig. 10 Comparison between predicted data with actual data of deviator stress using QM and MLR

Mathematical models

The developed mathematical models (MM) including QM and MLR were implemented to predict the deviator stress for the clay soil-NaOH mixtures. The data of clay soil content, NaOH content, LS, A, and F were used to generate a mathematical equation based on QM and MLR for q as given in Eqs. (8) and (9), respectively.

$$\begin{aligned} q = & -0.003054 - 0.000039 \bullet CSc \\ & - 0.000277 \bullet LS - 0.000147 \bullet A \\ & + 1.07364 \bullet F - 0.000770 \bullet CSc^2 \\ & - 0.005534 \bullet LS^2 + 0.003696 \bullet A^2 \\ & - 0.003347F^2 + 0.000809 \bullet CSc \bullet LS \\ & + 0.004298 \bullet CSc \bullet A - 0.001933 \bullet CSc \bullet F \\ & - 0.001844 \bullet LS \bullet A + 0.006123 \bullet LS \bullet F \\ & - 0.116304 \bullet A \bullet F, \end{aligned} \tag{8}$$

$$\begin{aligned} q = & 0.023284 - 0.005336 \bullet CSc \\ & + 0.006188 \bullet LS - 0.051475 \bullet A \\ & + 1.01040 \bullet F. \end{aligned} \tag{9}$$

Moreover, the results of the analysis of variance are presented in Table 4. The results of the actual data and the corresponding values predicted by Eqs. (7) and (9) are displayed in Fig. 10. To test the fit of the model, *R*-squared was determined. For higher modeling accuracy, the *R*-squared value should be closer to 1. In this case, the values of *R*-squared for training data are 0.99999 for QM and 0.9995 for MLR.

Moreover, Fig. 11 presents two-dimensional (2D) contour plots and three-dimensional (3D) surfaces for predicting the deviator stress of the treated soil. It shows the influence of

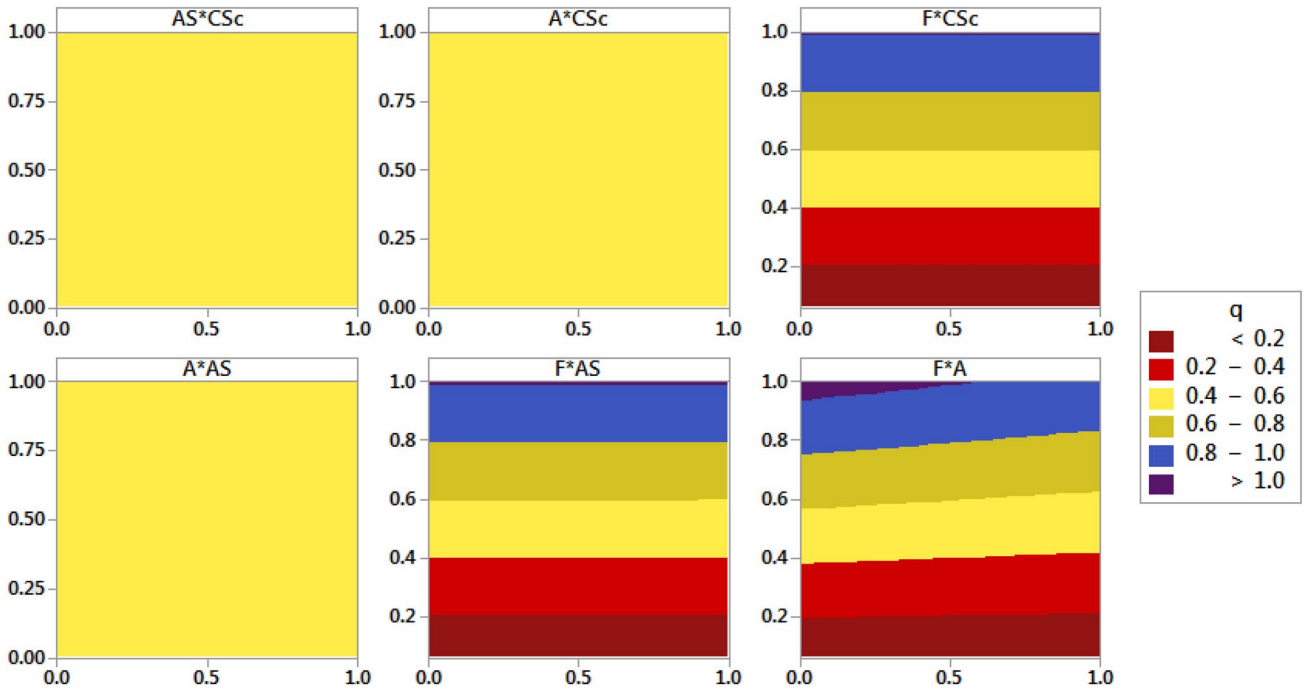

Fig. 11 Contour plots of deviator stress data

Table 5 Performance evaluation of the models

Statistical indicator	MFFNN	CFNN	RBFNN	ENN	QM	MLR
R-squared	0.9996	0.9939	0.9615	0.9977	0.9999	0.9994
RMSE	0.0041	0.0283	0.0575	0.0114	0.0035	0.0547
MAE	0.0013	0.0240	0.0322	0.0087	0.0029	0.0525
NSE	1.0000	0.7610	0.9110	0.9970	1.0000	0.9190
d	1.0000	0.9440	0.9800	0.9990	1.0000	0.9820

input variables (CSc, AS, *F*, *A*) on the deviator stress (*q*) of the treated soil. The number written on each contour area indicates the deviator stress in the specified conditions.

Performance evaluation of artificial models and mathematical models for testing data

The data were divided into training and testing groups and the results by the models were compared with each. In this study, the training was done using data for 0, 5, 10, and 20% NaOH treated soil, and the developed model was used to predict the stress–strain plot for 15% NaOH treated soil, and then compared with the stress–strain plot obtained by performing laboratory test on actually prepared 15% NaOH treated soil. Furthermore, the *R*-squared, RMSE, MAE, and ADD were determined to select the best model for predicting the behavior of stress–strain of clay soil-NaOH mixtures. *R*-squared is a measure of how well the regression line represents the data, while RMSE and MAE are direct methods for describing deviations. For high accuracy, *R*-squared must be close to 1.0, and the RMSE and MAE between the observed and predicted values must be as small as possible. Table 5 shows the results of the *R*-squared, RMSE, and MAE values for all models. It was observed that all models gave good predictions according to the *R*-squared values for the testing data. Also, it was found that the QM and MFFNN have the highest value of R^2 and the lowest value of RMSE and MAE for the testing data. Moreover, Fig. 12 shows the comparison of the estimated and observed values of the deviator stress for all models. Additionally, the values of deviator stress for CS15 are reported in Table S2 as supplementary material. The deviation between the estimated and experimental results of deviator stress is shown in Fig. 13. It can be seen that most of the deviations were positive and only a few were negative for QM and MFFNN models.

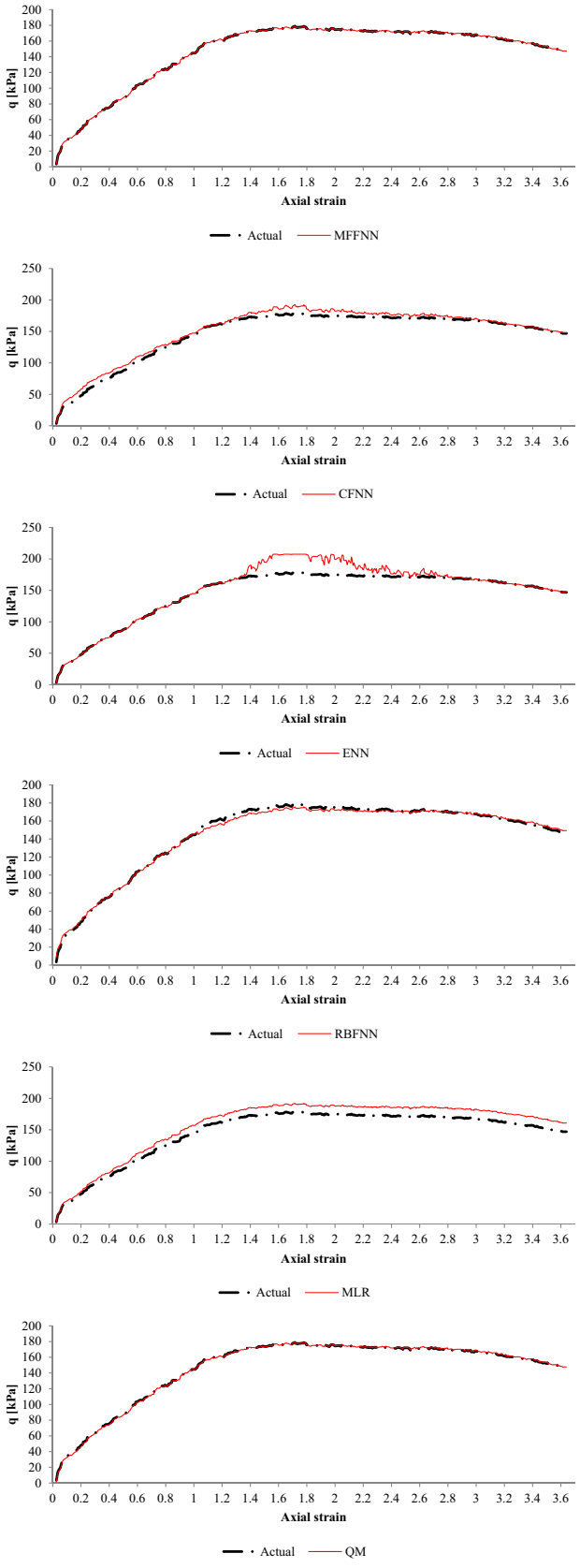

Fig. 12 Comparison of the predicted and observed values of the deviator stress of CS15 for all models

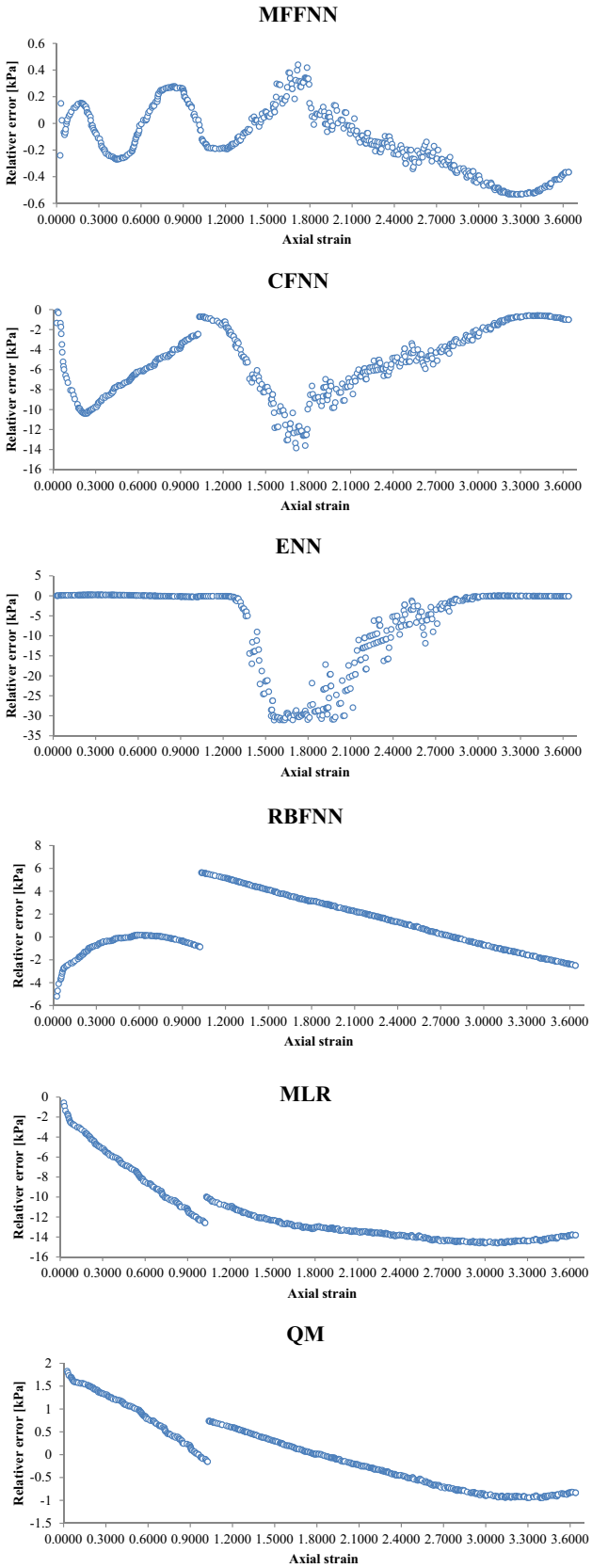

Fig. 13 The relative error for deviator stress

Conclusion

In this study, the effect of NaOH concentrations on the stabilization of high plasticity clay was investigated. Therefore, to address the main objective, the authors proposed a Quadratic model to predict the behavior of stress–strain of treated and untreated soil as a function of the percentage of clay soil, percentage of NaOH, axial strain (AS), area (A), and force (F). Besides, the behavior of stress–strain of soils was evaluated through four artificial models, namely Multilayer Feed-Forward Neural Network, Cascade Feed-forward Neural Network, Radial Basis Neural Network and Elman neural network based on the experimental data. Furthermore, the proposed models were then compared in terms of predictive accuracy to select the best model. The most important results can be summarized in the following cases:

- The treatment of studied soil with NaOH increases maximum dry unit weight and decreases the optimum moisture content.
- From the UCS test, it was observed that with increasing the percentage of NaOH from 0 to 15%, the peak axial stress increased from 97.54 to 201.71 kPa (i.e., the related maximum increment was up to 107%). Nevertheless, this value was reduced when the percentage of NaOH exceeded the optimum content of 15% NaOH. Similar trends were followed in the case of undrained shear strength values from stress–strain curves of UCS tests.
- Based on the stress–strain curves of UCS tests, it was observed that this treatment increases the stiffness and UCS of the soil without leading to considerable brittle behavior up to 15% addition of NaOH.
- The results indicate that the all developed models are valid in predicting the stress–strain behavior of treated soil. Furthermore, the findings demonstrated that the QM model performed well and presented high accuracy in modeling the stress–strain behavior.

Based on our findings, the QM model developed for this study to predict the stress–strain behavior of NaOH stabilized clay soil could be utilized further to test soil with other stabilizers or characteristics. Moreover, future research should focus on evaluating the effects of curing time on the engineering properties of the soil.

Supplementary Information The online version contains supplementary material available at https://doi.org/10.1007/s12665-022-10229-8.

Funding This research received no external funding.

Declarations

Conflict of interest The authors declare that they have no conflict of interest.

References

Abdeh A (2018) Mechanical behaviour of expansive clays in North Cyprus (master thesis). Near East University

Ahmad M, Hu JL, Ahmad F, Tang XW, Amjad M, Iqbal MJ et al (2021) Supervised learning methods for modeling concrete compressive strength prediction at high temperature. Materials 14(8):1983

Ahmad M, Tang X, Ahmad F (2020) Evaluation of liquefaction-induced settlement using random forest and REP tree models: taking pohang earthquake as a case of illustration. In: Natural hazards - impacts, adjustments and resilience. IntechOpen. https://doi.org/10.5772/intechopen.94274

Alkhasawneh MS, Tay LT (2018) A hybrid intelligent system integrating the cascade forward neural network with Elman neural network. Arab J Sci Eng 43(12):6737–6749

Asr AA, Faramarzi A, Javadi AA (2018) An evolutionary modelling approach to predicting stress-strain behaviour of saturated granular soils. Eng Comput 35(8):2931–2952. https://doi.org/10.1108/EC-01-2018-0025

Barati-Harooni A, Najafi-Marghmaleki A (2016) An accurate RBF-NN model for estimation of viscosity of nanofluids. J Mol Liq 224:580–588. https://doi.org/10.1016/j.molliq.2016.10.049

Coudert E, Paris M, Deneele D, Russo G, Tarantino A (2019) Use of alkali activated high-calcium fly ash binder for kaolin clay soil stabilisation: physicochemical evolution. Constr Build Mater 201:539–552. https://doi.org/10.1016/j.conbuildmat.2018.12.188

Cristelo N, Glendinning S, Miranda T, Oliveira D, Silva R (2012) Soil stabilisation using alkaline activation of fly ash for self compacting rammed earth construction. Constr Build Mater 36:727–735. https://doi.org/10.1016/j.conbuildmat.2012.06.037

Das B, Sobhan K (2014) Principles of geotechnical engineering, 8th edn. Cengage Learning, Florence, p 464

Davoudi M, Kabir E (2011) Interaction of lime and sodium chloride in a low plasticity fine grain soils. J Appl Sci 11(2):330–335. https://doi.org/10.3923/jas.2011.330.335

Debnath P, Dey AK (2016) Prediction of laboratory peak shear stress along the cohesive soil-geosynthetic interface using artificial neural network. Geotech Geol Eng 35(1):445–461. https://doi.org/10.1007/s10706-016-0119-2

Dutta R, Gnananandarao T, Ladol S (2020) Soft computing based predictionof friction angle of clay. Arch Mater Sci Eng 2(104):58–68. https://doi.org/10.5604/01.3001.0014.4895

Fasihnikoutalab MH, Pourakbar S, Ball RJ, Unluer C, Cristelo N (2019) Sustainable soil stabilisation with ground granulated blast-furnace slag activated by olivine and sodium hydroxide. Acta Geotech 15(7):1981–1991. https://doi.org/10.1007/s11440-019-00884-w

Ghadir P, Ranjbar N (2018) Clayey soil stabilization using geopolymer and Portland cement. Constr Build Mater 188:361–371. https://doi.org/10.1016/j.conbuildmat.2018.07.207

Ghavami S, Jahanbakhsh H, Azizkandi AS, Nejad FM (2020) Influence of sodium chloride on cement kiln dust-treated clayey soil: strength properties, cost analysis, and environmental impact. Environ Dev Sustain. https://doi.org/10.1007/s10668-020-00603-6

Gökçekuş H, Kassem Y, Aljamal J (2020) Analysis of different combinations of meteorological parameters in predicting rainfall with an ANN approach: a case study in Morphou, Northern Cyprus. Desalin Water Treat 177:350–362. https://doi.org/10.5004/dwt.2020.24988

Gokul V, Steffi DA, Kaviya R, Harni C, Dharani S (2020) Alkali activation of clayey soil using GGBS and NaOH. Mater Today. https://doi.org/10.1016/j.matpr.2020.10.044

Hassan HS, Abdel-Gawwad H, Vásquez-García S, Israde-Alcántara I, Flores-Ramirez N, Rico J, Mohammed MS (2019) Cleaner production of one-part white geopolymer cement using pre-treated wood biomass ash and diatomite. J Clean Prod 209:1420–1428. https://doi.org/10.1016/j.jclepro.2018.11.137

Hedayat A, Davilu H, Barfrosh AA, Sepanloo K (2009) Estimation of research reactor core parameters using cascade feed forward artificial neural networks. Prog Nucl Energy 51(6–7):709–718. https://doi.org/10.1016/j.pnucene.2009.03.004

Holtz K, Kovacs WD (1981) Kansas geotechnical survey, current research in earth science. Bulletin 244, part 3, The Relationship between Geology and Landslide Hazards of Atchison, Kansas and Vicinity

Hu M, Zhu X, Long F (2009) Alkali-activated fly ash-based geopolymers with zeolite or bentonite as additives. Cement Concr Compos 31(10):762–768. https://doi.org/10.1016/j.cemconcomp.2009.07.006

Javadi AA, Ahangar-Asr A, Johari A, Faramarzi A, Toll D (2012) Modelling stress–strain and volume change behaviour of unsaturated soils using an evolutionary based data mining technique, an incremental approach. Eng Appl Artif Intell 25(5):926–933

Jayawardane VS, Anggraini V, Li-Shen AT, Paul SC, Nimbalkar S (2020) Strength enhancement of geotextile-reinforced fly-ash-based geopolymer stabilized residual soil. Int J Geosynth Ground Eng. https://doi.org/10.1007/s40891-020-00233-y

Johari A, Javadi AA, Habibagahi G (2011) Modelling the mechanical behaviour of unsaturated soils using a genetic algorithm-based neural network. Comput Geotech 38(1):2–13

Kassem Y, Gökçekuş H, Çamur H (2018) Wind speed prediction of four regions in northern Cyprus prediction using ARIMA and Artificial Neural Networks models: a comparison study. In: 13th international conference on theory and application of fuzzy systems and soft computing—ICAFS-2018 advances in intelligent systems and computing. pp 230–238. https://doi.org/10.1007/978-3-030-04164-9_32

Kassem Y, Gökçekuş H, Çamur H (2019) Artificial neural networks for predicting the electrical power of a new configuration of Savonius rotor. In: Advances in intelligent systems and computing 10th international conference on theory and application of soft computing, computing with words and perceptions—ICSCCW-2019. pp 872–879. https://doi.org/10.1007/978-3-030-35249-3_116

Kassem Y, Gokcekus H (2021) Do quadratic and Poisson regression models help to predict monthly rainfall? Desalin Water Treat 215:288–318

Keat SC, Chun BB, San LH, Jafri MZ (2015) Multiple regression analysis in modelling of carbon dioxide emissions by energy consumption use in Malaysia. AIP Conf Proc. https://doi.org/10.1063/1.4915185

Kim HK, Lim Y, Tafesse M, Kim GM, Yang B (2022) Micromechanics-integrated machine learning approaches to predict the mechanical behaviors of concrete containing crushed clay brick aggregates. Constr Build Mater 317:125840

Kohestani VR, Hassanlourad M (2016) Modeling the mechanical behavior of carbonate sands using artificial neural networks and support vector machines. Int J Geomech 16(1):04015038

Livingstone DJ (2009) Artificial neural networks, vol 458. Springer, Berlin

Lyu H, Shen S, Yang J, Yin Z (2019) Inundation analysis of metro systems with the storm water management model incorporated into a geographical information system: a case study in Shanghai. Hydrol Earth Syst Sci 23(10):4293–4307. https://doi.org/10.5194/hess-23-4293-2019

Lyu H, Shen S, Zhou A, Chen K (2020) Calculation of pressure on the shallow-buried twin-tunnel in layered strata. Tunn Undergr Space Technol 103:103465. https://doi.org/10.1016/j.tust.2020.103465

Madhav S, Ahamad A, Singh P, Mishra PK (2018) A review of textile industry: wet processing, environmental impacts, and effluent treatment methods. Environ Qual Manage 27(3):31–41. https://doi.org/10.1002/tqem.21538

Miao S, Shen Z, Wang X, Luo F, Huang X, Wei C (2017) Stabilization of highly expansive black cotton soils by means of geopolymerization. J Mater Civ Eng 29(10):04017170

Modmoltin C, Voottipruex P (2009) Influence of salts on strength of cement-treated clays. Proc Inst Civ Eng 162(1):15–26. https://doi.org/10.1680/grim.2009.162.1.15

Mohanty S (2018) Stabilization of expansive soil using industrial waste: fly ash. Civ Eng Res J. https://doi.org/10.19080/cerj.2018.03.555606

Molaabasi H, Saberian M, Kordnaeij A, Omer J, Li J, Kharazmi P (2019) Predicting the stress-strain behaviour of zeolite-cemented sand based on the unconfined compression test using GMDH type neural network. J Adhes Sci Technol 33(9):945–962. https://doi.org/10.1080/01694243.2019.1571659

Murmu AL, Dhole N, Patel A (2020) Stabilisation of black cotton soil for subgrade application using fly ash geopolymer. Road Mater Pavement Des 21(3):867–885

Murray HH (2007) Applied clay mineralogy: occurrences, processing and applications of kaolins, bentonites, palygorskitesepiolite, and common clays. Elsevier, Amsterdam

Nassr A, Esmaeili-Falak M, Katebi H, Javadi A (2018) A new approach to modeling the behavior of frozen soils. Eng Geol 246:82–90. https://doi.org/10.1016/j.enggeo.2018.09.018

Neeladharan C, Vinitha V, Priya B, Saranya S (2007) Stabilisation of soil by using tiles waste with sodium hydroxide as binder. Int J Innov Res Sci Eng Technol 6(4):6762–6768

Parhi PS, Garanayak L, Mahamaya M, Das SK (2017) Stabilization of an expansive soil using alkali activated fly ash based geopolymer. Sustain Civ Infrastruct Adv Characteriz Anal Expans Soils Rocks. https://doi.org/10.1007/978-3-319-61931-6_4

Pham K, Jung S, Park S, Kim D, Choi H (2022) Bayesian neural network for estimating stress-strain behaviors of frozen sand. KSCE J Civ Eng 26(2):933–941

Phummiphan I, Horpibulsuk S, Sukmak P, Chinkulkijniwat A, Arulrajah A, Shen S (2016) Stabilisation of marginal lateritic soil using high calcium fly ash-based geopolymer. Road Mater Pavement Des 17(4):877–891. https://doi.org/10.1080/14680629.2015.1132632

Phummiphan I, Horpibulsuk S, Phoo-Ngernkham T, Arulrajah A, Shen S (2017) Marginal lateritic soil stabilized with calcium carbide residue and fly ash geopolymers as a sustainable pavement base material. J Mater Civ Eng 29(2):04016195. https://doi.org/10.1061/(asce)mt.1943-5533.0001708

Rai P, Pei H, Meng F, Ahmad M (2020) Utilization of marble powder and magnesium phosphate cement for improving the engineering characteristics of soil. Int J Geosynth Ground Eng 6:1–13

Rashad AM, Zeedan SR (2011) The effect of activator concentration on the residual strength of alkali-activated fly ash pastes subjected to thermal load. Constr Build Mater 25(7):3098–3107. https://doi.org/10.1016/j.conbuildmat.2010.12.044

Ren G, Cao Y, Wen S, Huang T, Zeng Z (2018) A modified Elman neural network with a new learning rate scheme. Neurocomputing 286:11–18

Shalabi FI, Asi IM, Qasrawi HY (2017) Effect of by-product steel slag on the engineering properties of clay soils. J King Saud Univ 29(4):394–399. https://doi.org/10.1016/j.jksues.2016.07.004

Siddiqui FI, Osman SB (2012) Simple and multiple regression models for relationship between electrical resistivity and various soil

properties for soil characterization. Environ Earth Sci 70(1):259–267. https://doi.org/10.1007/s12665-012-2122-0

Tanegonbadi B, Noorzad R (2017) Stabilization of clayey soil using lignosulfonate. Transp Geotech 12:45–55. https://doi.org/10.1016/j.trgeo.2017.08.004

Yao Y, Zheng J, Zhang J, Peng J, Li J (2018) Model for predicting resilient modulus of unsaturated subgrade soils in south China. KSCE J Civ Eng 22(6):2089–2098. https://doi.org/10.1007/s12205-018-1703-1

Yu C, Li Y, Zhang M (2017) Comparative study on three new hybrid models using Elman neural network and empirical mode decomposition based technologies improved by singular spectrum analysis for hour-ahead wind speed forecasting. Energy Convers Manage 147:75–85

Yu D, Wang Y, Liu H, Jermsittiparsert K, Razmjooy N (2019) System identification of PEM fuel cells using an improved Elman neural network and a new hybrid optimization algorithm. Energy Rep 5:1365–1374

Zhang N, Shen JS, Lin C, Arulrajah A, Chai J (2017) Investigation of a large ground collapse and countermeasures during mountain tunnelling in Hangzhou: a case study. Bull Eng Geol Env 78(2):991–1003. https://doi.org/10.1007/s10064-017-1098-0

Zhang N, Shen SL, Zhou A, Jin YF (2021) Application of LSTM approach for modelling stress–strain behaviour of soil. Appl Soft Comput 100:106959

Zheng Y, Shadloo MS, Nasiri H, Maleki A, Karimipour A, Tlili I (2020) Prediction of viscosity of biodiesel blends using various artificial model and comparison with empirical correlations. Renew Energy 153:1296–1306. https://doi.org/10.1016/j.renene.2020.02.087